

## RESEARCH ARTICLE

10.1029/2018JC014306

## Key Points:

- Potential spicity function is defined in terms of a least square minimization problem, which is solved by a two-step linearization method
- Potential spicity is defined for EOS-80 and TEOS\_10, with angle deviation from orthogonality on the order of  $0.0001^\circ$
- Potential spicity and potential density consist of an orthogonal coordinate system, which provides a new tool in water mass analysis

## Supporting Information:

- Supporting Information S1

## Correspondence to:

S.-Q. Zhou,  
sqzhou@scsio.ac.cn

## Citation:

Huang, R. X., Yu, L.-S., & Zhou, S.-Q. (2018). New definition of potential spicity by the least square method. *Journal of Geophysical Research: Oceans*, 123, 7351–7365. <https://doi.org/10.1029/2018JC014306>



Received 25 JUN 2018

Accepted 28 SEP 2018

Accepted article online 2 OCT 2018

Published online 16 OCT 2018

## New Definition of Potential Spicity by the Least Square Method

Rui Xin Huang<sup>1</sup> , Lu-Sha Yu<sup>2,3</sup>, and Sheng-Qi Zhou<sup>2,3</sup> 

<sup>1</sup>Woods Hole Oceanographic Institution, Woods Hole, MA, USA, <sup>2</sup>State Key Laboratory of Tropical Oceanography, Guangzhou, China, <sup>3</sup>University of Chinese Academy of Sciences, Beijing, China

**Abstract** A differentiable function whose contours are orthogonal to potential density ( $\sigma$ ) contours does not exist. However, such a function, called potential spicity ( $\pi$ ), can be defined in the least square sense; these two functions form a practically orthogonal coordinate system in potential temperature-salinity ( $\theta$ - $S$ ) space. Thus, in addition to the classical potential temperature-salinity ( $\theta$ - $S$ ) diagram, seawater properties can be studied in the potential density-potential spicity ( $\sigma - \pi$ ) diagram.

**Plain Language Summary** Potential spicity is defined in the least square sense, forming a practically orthogonal coordinate system with the potential density in potential temperature-salinity ( $\theta$ - $S$ ) space, which can be used to study seawater properties.

## 1. Introduction

The concept of a thermodynamic variable whose contours are *orthogonal* to potential density contours in the potential temperature-salinity ( $\theta$ - $S$ ) space has been discussed in many previous publications, for example, Stommel (1962), Mamayev (1975), Veronis (1972), and Munk (1981). The orthogonality between this variable and potential density is very important because this variable can describe temperature and salinity information not included in potential density (Veronis, 1972).

In the early study by Veronis (1972), the concept of constructing a curvilinear coordinates system based on potential density and potential spicity, which is orthogonal in the  $\theta - S$  plane, was first proposed. Mamayev (1975) went through a lengthy discussion about the advantage of introduction of such orthogonal coordinates. Munk (1981) proposed to name such a thermodynamic variable as *spiciness*, whose contours are orthogonal to potential density contours; he argued that the variety of such a variable along the isopycnals should “give a measure of the strength of the intrusion.”

Jackett and McDougall (1985) demonstrated that in theory a differential function whose contours are exactly orthogonal to those of potential density does not exist; this theoretical argument will be followed up in detail shortly. Therefore, they abandoned the orthogonality constraint postulated by pioneers in the searching of such function in previous studies. Their approach was following up in the subsequent studies, such as Flament (2002) and McDougall and Krzysik (2015).

Note that in most previous studies, such as Flament (2002), Huang (2011), and McDougall and Krzysik (2015), the term spiciness or *spicity* has been used in the paper titles and through most part of text. For water mass analysis, it is much more accurate to call this function as the potential spicity ( $\pi$ ), whose contours are orthogonal to those of the potential density referenced to the same pressure. Thus, throughout this whole paper, a more accurate terminology, potential spicity, is adapted and its application to the water mass analysis is discussed briefly.

Similar to Jackett and McDougall (1985), McDougall and Krzysik (2015) “have opted to have the isopycnal variations of spiciness be proportional to the isopycnal water-mass variations, expressed in terms of density. Because of the nonlinear nature of the equation of state of seawater, this water-mass variation constraint cannot be simultaneously satisfied with any definition of orthogonality. We have argued that there is no theoretical justification for any meaning of orthogonality”. Flament (2002) postulated a spiciness function whose contours have slope of the same magnitude as those of the potential density, but the signs are opposite in the  $\theta$ - $S$  diagram. Flament did not discuss the technical details associated with solving the nonlinear least square problem in his approach.

The debate about how to define a useful thermodynamic variable in addition to the potential density has been focused on two issues. First, whether we can define a thermodynamic variable whose contours are

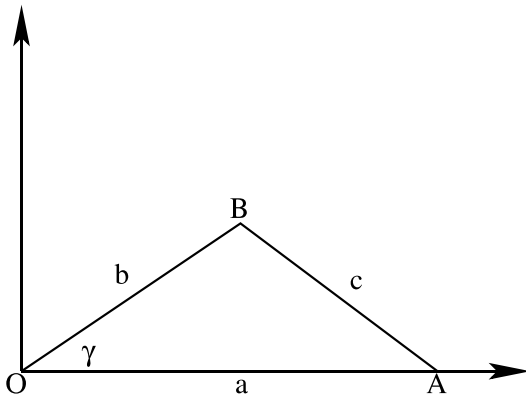


**Figure 1.** An example for a triangle in a rectangular plane.

orthogonal to potential density contours. Second, what is the physical meaning and advantage of such a function. The first question has no positive answer up till now. Despite several attempts, no potential spicity function satisfying the orthogonality constraint has been found. Regarding the second question, although Veronis (1972) and Mamayev (1975) theorized that the orthogonality makes it possible to construct a new orthogonal coordinates for water mass study, since such a function was not available for a long time, no specific advantages of using such a potential spicity function have been discussed. Thus, up till now most studies are based on the nonorthogonal functions, for example, the spiciness function postulated by Flament (2002) and McDougall and Krzysik (2015). Huang (2011) tried to define a potential spicity function whose contours are orthogonal to those of potential density; however, the defined function is not really orthogonal, as will be shown shortly. Without orthogonality, the physical meaning of potential spicity would be less clear. For example,

it would be impossible for potential spicity acting as the density flux function as proposed by Mamayev (1975).

The main goal of this study is to define a potential spicity function whose contours are orthogonal to the potential density contours in the least square sense. Note that the orthogonality we defined here is based on a fixed aspect ratio of the axes; if the aspect ratio of the axes is changed, any orthogonal coordinates will become nonorthogonal; thus, this definition of orthogonal depends on the relative scales chosen for the axes of the  $\theta - S$  diagram, similar to Veronis (1972). The advantages of the orthogonal coordinates are fairly obvious: both coordinates can be regarded as independent.

That the orthogonal coordinate system is superior to the nonorthogonal ones can be clearly illustrated in the following example. From the basic formula in trigonometry, the lengths of the three sides of a triangle in Figure 1 satisfy the following relation

$$c^2 = a^2 + b^2 - 2ab \cos \gamma. \quad (1)$$

Thus, the distance between two points A and B in a plane satisfies the above equation. Hence,  $c^2 \leq a^2 + b^2$ , and the equal sign holds only when  $\gamma = 90^\circ$ , that is, when OB is orthogonal to OA. This is the common knowledge that the distance between two points satisfies the simple relation  $c^2 = a^2 + b^2$  if and only if the coordinate system is an orthogonal system.

In general, in orthogonal coordinates the signals can be separated into two components to the maximum degree. For example, orthogonal coordinates have no off-diagonal terms in their metric tensor, such as the  $2ab \cos \gamma$  term in the equation above. In other words, the infinitesimal squared distance can always be written as the sum of the squared infinitesimal coordinate displacements.

This paper is organized as follows. In section 2, we review the different approaches used in defining potential spicity function. Since a scalar function whose contours are exactly orthogonal to those of potential density does not exist in theory, we modify our goal in section 3, where a least square problem in terms of the root-mean-square (RMS) angle deviation from the orthogonality is defined. However, this is a nonlinear least square problem with multiple parameters, which is hard to solve directly. We propose a two-step approach. In section 3, the original problem is modified as the searching of a scalar function whose gradient matches the target vector obtained by rotating the gradient vector of potential density by  $90^\circ$ . In section 4, the solution is further improved by searching the solutions of a linearized nonlinear least square problem. Using the solution obtained by the method discussed in section 3 as the initial solution, the final solution is obtained through iteration. Potential spicity functions at different reference pressure levels are defined by applying these methods to the previous version of equation of state, UNESCO EOS-80 in section 5 and the most updated version of UNESCO TEOS\_10 in section 6. These potential spicity functions can be used as tools in the study of oceanography. As an example, we discuss the concept of radius of signal and its application to a pair of station along the equatorial Pacific Ocean in section 7. Finally, we give a conclusion in Section 8.

## 2. Define Potential Spicity by Line Integration

First of all, in order to define the so-called function perpendicular or orthogonal to each other for two families of contours, we must use the same dimension for both axes of the  $\theta - S$  diagram, so that we can compare gradients at different directions in the  $\theta - S$  space. Furthermore, a square grid box in such a phase space should have the same length in the same unit. It is to emphasize that the orthogonality discussed in this study is meaningful only for a fixed aspect ratio between the horizontal and vertical axis lengths. Therefore, we will use the following pair of variables. Most importantly, they have the same dimensions as the potential density

$$x = \rho_0 \beta_0 S, \frac{\partial}{\partial x} = \frac{1}{\rho_0 \beta_0} \frac{\partial}{\partial S}, \quad y = \rho_0 \alpha_0 \theta, \frac{\partial}{\partial y} = \frac{1}{\rho_0 \alpha_0} \frac{\partial}{\partial \theta}, \quad (2)$$

where  $\alpha_0 = \bar{\alpha}$  and  $\beta_0 = \bar{\beta}$  are the mean values of thermal expansion and saline contraction coefficients averaged on the domain of  $\theta = [-2, 40](^{\circ}\text{C})$  and  $S = [10, 40]$ (practical salinity units, psu). In this coordinates the potential density gradient operator equals to

$$\nabla \sigma = \vec{i} \frac{\partial \sigma}{\partial x} + \vec{j} \frac{\partial \sigma}{\partial y} = \vec{i} \frac{1}{\rho_0 \beta_0} \frac{\partial \sigma}{\partial S} + \vec{j} \frac{1}{\rho_0 \alpha_0} \frac{\partial \sigma}{\partial \theta} = \vec{i} \frac{\beta}{\beta_0} - \vec{j} \frac{\alpha}{\alpha_0}. \quad (3)$$

On the sea surface, the net pressure is zero,  $p = 0$ , thus the thermodynamic state of seawater can be expressed in terms of two variables ( $\theta, S$ ). In the traditional way, potential density is used as a dynamical variable, the best choice of the other thermodynamic variable should be called potential spicity, which varies along the potential density isopleths and it is denoted as  $\pi$ . There are many choices for this thermodynamic variable. One of the choices discussed in previous studies is the requirement that the gradients of potential density and potential spicity are perpendicular

$$\nabla \sigma \cdot \nabla \pi = 0. \quad (4)$$

A simple way to construct such a function is to define it as follows,

$$\pi_x = -\sigma_y, \pi_y = \sigma_x. \quad (5)$$

If we can find such a function, and it is differentiable twice, then it is readily seen that the vector field associated with the gradient of potential spicity is nondivergent, that is,

$$\nabla \cdot (\nabla \pi) = 0. \quad (6)$$

From equation (6), one can derive the following constraint,

$$\nabla \cdot (\nabla \sigma) = \nabla \cdot (\pi_y \vec{i} - \pi_x \vec{j}) = \sigma_{xx} + \sigma_{yy} = 0. \quad (7)$$

The left hand side of this equation may be called the *source* of potential density. As shown in Figure 2, the commonly used function of potential density does not satisfy such a constraint. The source is primarily due to the second term contribution associated with the increase of thermal expansion coefficient with temperature. At low salinity and low temperature, the first term of the source is quite large compared with its mean value, and this is the major obstacle in constructing the desirable potential spicity function orthogonal to potential density.

In general, a vector  $\vec{g} = (g^x, g^y)$  is called a conserved vector when its components satisfy the constraint:  $\partial g^y / \partial x = \partial g^x / \partial y$ . For a conserved vector, there exists a scalar function  $H(x, y)$ , whose gradient equals this vector, that is,  $\nabla H(x, y) = \vec{g}$ . The construction of such a scalar function can be carried out by the integration of  $H(x, y)$  along chosen paths, and the results are independent of the choice of the integral path.

However, if the constraint  $\partial g^y / \partial x = \partial g^x / \partial y$  is not satisfied, a differentiable function which satisfies constraint  $\nabla H(x, y) = \vec{g}$  does not exist. In such a case, although one can construct a function by integrating the differential relation along certain selected paths, the results do not lead to a differentiable function. Most importantly, the results of such integration will depend on the selected paths. Therefore, potential spicity (spiciness) functions obtained by following different integral paths are different, and they should also have different physical meanings.

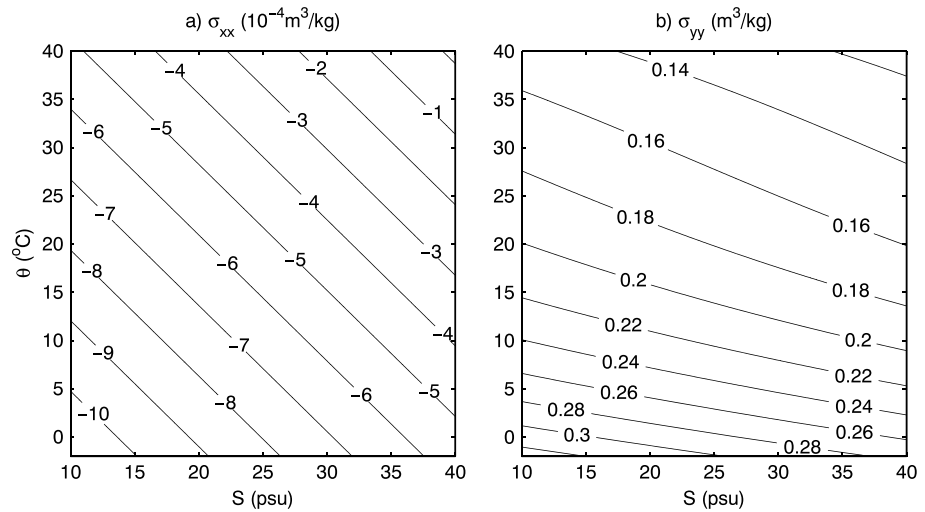


**Figure 2.** The source terms, shown in equation (7), of the seawater potential density at sea surface pressure. psu = practical salinity unit.

Since potential density satisfies the differential relation

$$\nabla\sigma = \rho_0(-\alpha\nabla\theta + \beta\nabla S), \tag{8}$$

the desirable potential spicity function should satisfy the differential relation

$$\nabla\pi = \rho_0 c(\theta, S)(\beta\nabla\theta + \alpha\nabla S) \tag{9}$$

where  $c(\theta, S)$  is an arbitrary function. In previous studies, a slightly different differential relation was used

$$\nabla\pi = \rho_0(\alpha\nabla\theta + \beta\nabla S). \tag{10}$$

Note that a function satisfies (10) is not orthogonal to density. A lot of efforts have been focused on finding the solution by projecting constraint (10) onto certain curves and calculating the potential spicity function by line integration. For example, Huang (2011) postulated the following method. First, the potential spicity function is defined along a constant salinity line  $S = S_0$ . Second, starting from this constant salinity line potential spicity function is constructed by projecting relation (10) onto each constant temperature line, black lines with arrows in Figure 3

$$\Delta\pi = \rho_0 \int_{S_0}^S \beta|_{\theta=const.} dS. \tag{11}$$

Using the approach by Jackett and McDougall (1985), McDougall and Krzysik (2015) used the following method. First, the spiciness function is defined along a constant temperature line  $\theta = \theta_0$ . Second, along each constant potential density contour (blue curves with arrows in Figure 3),  $\nabla\sigma = 0$ . Thus, the spiciness function is constructed by starting from this constant temperature line and projecting relation (10) onto each constant potential density contour, blue lines with arrows in Figure 3

$$\Delta\pi = 2\rho_0 \int_{S_0}^S \beta|_{\sigma=const.} dS. \tag{12}$$

Similarly, one can also construct another spiciness function as follows. As the first step, the spiciness function is defined along a constant

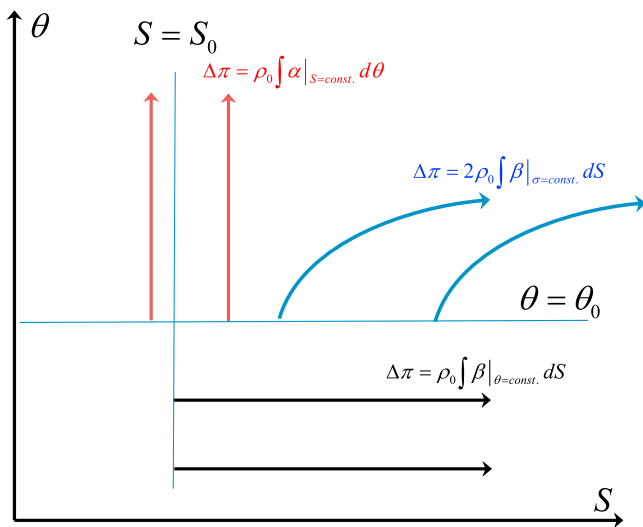


**Figure 3.** Selected integral paths for defining potential spicity function in the  $\theta - S$  space. Paths marked as black, blue, and red arrowed lines have been used in Huang (2011), Jackett and McDougall (1985), and McDougall and Krzysik (2015), and a similar method, respectively.

temperature line  $\theta = \theta_0$ . Afterward, spiciness function is constructed by projecting relation (10) onto each constant salinity line, red lines with arrows in Figure 3

$$\Delta\pi = \rho_0 \int_{S_0}^S \alpha|_{S=\text{const}} d\theta. \quad (13)$$

As discussed above, the potential spicity (spiciness) functions constructed through these different integral paths must be different. Most importantly, although the potential spicity function satisfies the constraints obtained by projecting the exact differential relation (10) onto the integral path, such functions do not satisfy the original differential relations in directions other than the tangent of the integral path. Thus,  $\nabla\pi \neq \rho_0(\alpha\nabla\theta + \beta\nabla S)$  in general; in particular, potential spicity function contours are not orthogonal to the potential density contours. As such, the meaning of such defined potential spicity functions remains unclear. In fact, although potential spicity had been used in many studies in the past, the physical meanings of this variable remain poorly understood.

### 3. Define Potential Spicity in the Least Square Sense

As discussed above, a scalar function which exactly satisfies constraint (4) does not exist. However, we can slightly modify our goal of the exact orthogonality as follows. By definition, the angle between  $\nabla\sigma$  and  $\nabla\pi$  is  $\lambda = \arccos\left(\frac{\nabla\sigma \cdot \nabla\pi}{|\nabla\sigma||\nabla\pi|}\right)$ , and the *nonorthogonality* can be measured in terms of the deviation from the target value of  $90^\circ$ . We will search a function  $\pi(x, y)$  which can satisfy constraint (4) in the least square sense over the domain of  $\theta$ - $S$  diagram, that is,

$$\Delta\lambda = \text{RMS}\left[\arcsin\left(\frac{\nabla\sigma \cdot \nabla\pi}{|\nabla\sigma||\nabla\pi|}\right)\right] = \text{Minimum}. \quad (14)$$

In the common practice, seawater properties are defined in terms of high-order polynomials, the task defined by equation (14) is a least square problem in multivariables, with up to tens of variables. Such a nonlinear least square problem is rather difficult to be solved. We will solve this least square problem in two steps.

First, a target vector  $(-\sigma_y, \sigma_x)$  is created by rotating the gradient vector  $\nabla\sigma$ ; our goal is to search a scalar function  $\pi$ , the components of whose gradient vector match the lengths of this target vector. As discussed above, it is impossible to find a perfect match. Therefore, we modify our goal as follows: searching for a scalar function  $\pi$ , whose gradient vector match the length of the target vector in the least square sense.

$$\Delta R = \text{RMS}\left((\pi_x + \sigma_y)^2 + (\pi_y - \sigma_x)^2\right) = \text{Minimum}. \quad (15)$$

We will denote this scalar target function for  $\pi$  as  $f$  and will choose to fit this function in terms of a polynomial. To illustrate the basic idea, we use a fourth order polynomial in the following discussion; hence, our goal is to define the following fitting function,  $f$ , as

$$f = a_1x + a_2y + a_3x^2 + a_4xy + a_5y^2 + a_6x^3 + a_7x^2y + a_8xy^2 + a_9y^3 + a_{10}x^4 + a_{11}x^3y + a_{12}x^2y^2 + a_{13}xy^3 + a_{14}y^4, \quad (16)$$

where  $a_k$  ( $k = 1, 2, 3, \dots, 14$ ) is the fitting coefficients to be fixed. This function can be used to calculate the potential spicity at each grid point  $(i, j)$  in the  $\theta$ - $S$  diagram. We assume that the vector  $\vec{A} = (A_{i,j}^x, A_{i,j}^y) = (-\sigma_{i,j}^y, \sigma_{i,j}^x)$  perpendicular to potential density is given for each grid point. We introduce the following notations

$$\begin{aligned} dx &= x_{i+1} - x_{i-1}, dy = y_{j+1} - y_{j-1}, \Delta x_i^2 = x_{i+1}^2 - x_{i-1}^2, \Delta y_j^2 = y_{j+1}^2 - y_{j-1}^2, \\ \Delta x_i^3 &= x_{i+1}^3 - x_{i-1}^3, \Delta y_j^3 = y_{j+1}^3 - y_{j-1}^3, \Delta x_i^4 = x_{i+1}^4 - x_{i-1}^4, \Delta y_j^4 = y_{j+1}^4 - y_{j-1}^4. \end{aligned} \quad (17)$$

Using the central difference scheme, we have the following finite differences

$$\begin{aligned} \Delta f_{i,j}^x = & a_1 dx + a_3 \Delta x_i^2 + a_4 y_j dx + a_6 \Delta x_i^3 + a_7 y_j \Delta x_i^2 + a_8 dx y_j^2 \\ & + a_{10} \Delta x_i^4 + a_{11} \Delta x_i^3 y_j + a_{12} \Delta x_i^2 y_j^2 + a_{13} dx y_j^3, \end{aligned} \quad (18)$$

$$\begin{aligned} \Delta f_{i,j}^y = & a_2 dy + a_4 x_i dy + a_5 \Delta y_j^2 + a_7 x_i^2 dy + a_8 x_i \Delta y_j^2 + a_9 \Delta y_j^3 \\ & + a_{11} x_i^3 dy + a_{12} x_i^2 \Delta y_j^2 + a_{13} x_i \Delta y_j^3 + a_{14} \Delta y_j^4. \end{aligned} \quad (19)$$

Our goal is to fit the given vector  $\vec{A} = (A_{i,j}^x, A_{i,j}^y)$ . For the  $x$ -component of the vector, ideally we should have

$$\Delta f_{i,j}^x = X_{i,j}, \quad \text{where } X_{i,j} = dx \cdot A_{i,j}^x. \quad (20)$$

Thus, the corresponding error in fitting this component of the vector is

$$\varepsilon^x = \Delta f_{i,j}^x - X_{i,j}. \quad (21)$$

Similarly, the errors in fitting the other component of the vector is

$$\varepsilon^y = \Delta f_{i,j}^y - Y_{i,j}, \quad \text{where } Y_{i,j} = dy \cdot A_{i,j}^y. \quad (22)$$

Therefore, the target of least square problem (15) is to minimize the following function

$$E = \left( \Delta f_{i,j}^x - X_{i,j} \right)^2 + \left( \Delta f_{i,j}^y - Y_{i,j} \right)^2. \quad (23)$$

The constraints of minimizing this target function are

$$\delta E / \delta a_k = 0, \quad k = 1, 2, 3, \dots, 14. \quad (24)$$

For example, at grid  $(i, j)$  the first constraint  $\delta E / \delta a_1 = 0$  leads to

$$\left( \Delta f_{i,j}^x - X_{i,j} \right) dx = 0. \quad (25)$$

Summarize over all grids leads to the following equation

$$\sum_{i,j} \Delta f_{i,j}^x dx = \sum_{i,j} X_{i,j} dx, \quad (26)$$

where the left-hand side is a linear function of  $a_k$  ( $k = 1, 2, 3, \dots, 14$ ).

The second example is for the constraint  $\delta E / \delta a_7 = 0$ . At a grid  $(i, j)$  this constraint leads to

$$\Delta f_{i,j}^x \Delta x_i^2 y_j + \Delta f_{i,j}^y x_i^2 dy = X_{i,j} \Delta x_i^2 y_j + Y_{i,j} x_i^2 dy. \quad (27)$$

Summarizing over all grids leads to

$$\sum_{i,j} \left( \Delta f_{i,j}^x \Delta x_i^2 y_j + \Delta f_{i,j}^y x_i^2 dy \right) = \sum_{i,j} \left( X_{i,j} \Delta x_i^2 y_j + Y_{i,j} x_i^2 dy \right), \quad (28)$$

where the left-hand side is a linear function of  $a_k$  ( $k = 1, 2, 3, \dots, 14$ ).

The final set of linear equations for the coefficients  $a_k$  ( $k = 1, 2, 3, \dots, 14$ ) is

$$F \cdot \vec{a} = \vec{e}, \quad (29)$$

where  $F$  is a  $14 \times 14$  matrix, both  $\vec{a}$  and  $\vec{e}$  are 14-dimensional vectors; the construction of both  $F$  and  $\vec{e}$  are discussed above. From equation (29), we can calculate vector  $\vec{a}$  by simply inverting the matrix  $F$

$$\vec{a} = F^{-1} \cdot \vec{e}. \quad (30)$$

With the vector  $\vec{a}$  calculated, the potential spicity function in terms of a fourth order polynomial is completely determined.

Although the result of this calculation gives us a fitting function  $f$ , whose gradient vector satisfies the least square constraint (15), the error of angle deviation from orthogonality is still rather large. Thus, such a scalar function is not the desirable solution for the least square problem (14). In order to find solution with smaller angle deviation from orthogonality, at the second step we will use an iteration process to solve the original least square problem (14), and the solution obtained from solving least square problem (15) can be used as a good candidate for initial solution at the beginning of the iteration process discussed below.

#### 4. Solve the Linearized Least Square Problem

For small angle, the least square problem defined in equation (14) can be reduced to

$$\Delta\lambda = RMS\left(\frac{\nabla\sigma}{|\nabla\sigma|} \cdot \frac{\nabla\pi}{|\nabla\pi|}\right) = Minimum. \quad (31)$$

Directly solving this nonlinear least square problem is difficult. However, this problem can be further reduced to the following linear least square problem

$$\Delta\lambda = RMS\left(\frac{\nabla\sigma \cdot \nabla\pi}{|\nabla\sigma| |\nabla\pi_0|}\right) = Minimum, \quad (32)$$

where  $\pi_0$  is the initial result of the approximate potential spicity function obtained in the previous iteration and  $\pi$  is the potential spicity function calculated as the new corrected solution. In fact, the solution obtained from equation (29) can be used as a good first initial solution.

The target function of the problem defined in equation (32) is

$$C = \frac{1}{R} (\sigma_x \pi_x + \sigma_y \pi_y)^2, R = (\sigma_x^2 + \sigma_y^2) (\pi_{0,x}^2 + \pi_{0,y}^2). \quad (33)$$

Following the notation used in the previous section, we have

$$\pi_x = \Delta f_{ij}^x / 2\Delta x, \pi_y = \Delta f_{ij}^y / 2\Delta y. \quad (34)$$

The constraints of minimizing this target function are

$$\delta C / \delta a_k = 0, k = 1, 2, 3, \dots, 14. \quad (35)$$

For example, this constraint upon the first parameter,  $a_1$ , leads to an equation

$$0 = \delta C / \delta a_1 = \frac{2}{R} (\sigma_x \pi_x + \sigma_y \pi_y) \left( \frac{\sigma_x}{2\Delta x} \delta \Delta f_{i,j}^x / \delta a_1 + \frac{\sigma_y}{2\Delta y} \delta \Delta f_{i,j}^y / \delta a_1 \right) \quad (36)$$

or  $\frac{\sigma_x}{R\Delta x} (\sigma_x \pi_x + \sigma_y \pi_y) dx = 0.$

This relation should apply to each grid point, and the summation over all grid points leads to the following equation

$$\sum_{i,j} \frac{\sigma_x}{R\Delta x} (\sigma_x \pi_x + \sigma_y \pi_y) dx = 0. \quad (37)$$

Note that  $R$  in the denominator is specified from the previous iteration;  $\pi_x$  &  $\pi_y$  in  $(\sigma_x \pi_x + \sigma_y \pi_y)$  is treated as unknown; thus, they are the linear function of unknown  $a_k$  ( $k = 1, 2, 3, \dots, 14$ ).

Similarly, we obtain the corresponding equations for parameter  $a_2, a_3, \dots, a_{14}$ . In this way, we obtain one set of equations system of 14 variables  $a_k$  ( $k = 1, 2, 3, \dots, 14$ ) and 14 equations, similar to equation (29).

$$\begin{bmatrix} b_{1,1} & b_{1,2} & \dots & b_{1,14} \\ b_{2,1} & b_{2,2} & \dots & b_{2,14} \\ \dots & \dots & \dots & \dots \\ b_{14,1} & b_{14,2} & \dots & b_{14,14} \end{bmatrix} \begin{pmatrix} a_1 \\ a_2 \\ \dots \\ a_{14} \end{pmatrix} = 0, \quad (38)$$

where the matrix  $B = (b_{ij})$  is defined in a way similar to the procedure leading to equation (29) discussed above. However, the right hand side of this equation system is zero; thus, the only solution is trivial of zero. To find meaningful solutions we choose the following iterative approach, and solutions obtained from the linear least square problem defined in equation (29) can be used as the first initial solution.

The original equation system (38) is separated into two parts. First, we rewrite the first equation in the following form

$$a_1^1 = -(b_{1,2}a_2^0 + b_{1,3}a_3^0 + \dots + b_{1,14}a_{14}^0)/a_{11}. \quad (39)$$

Using  $(a_2^0, a_3^0, \dots, a_{14}^0)$  from the previous solution, we can calculate  $a_1^1$ , the first parameter of the new solution. When this new value  $a_1^1$  is obtained, we can calculate the new values of other parameters by using the following equation system, which is a subset of the original equation system (38)

$$\begin{bmatrix} b_{2,2} & b_{2,3} & \dots & b_{2,14} \\ b_{23,2} & b_{3,3} & \dots & b_{3,14} \\ \dots & \dots & \dots & \dots \\ b_{14,2} & b_{14,3} & \dots & b_{14,14} \end{bmatrix} \begin{pmatrix} a_2^1 \\ a_3^1 \\ \dots \\ a_{14}^1 \end{pmatrix} = -a_1^1 \begin{pmatrix} b_{2,1} \\ b_{3,1} \\ \dots \\ b_{14,1} \end{pmatrix}. \quad (40)$$

Solving this equation can lead to an improved solution with smaller RMS of the angle errors over the  $\theta$ - $S$  diagram. This approach can be applied iteratively. Since the original least square problem is defined of a multi-dimensional parameter space, there occur many solutions corresponding to localized minima in the parameter space; among these solutions we choose the one with the smallest RMS error of angle deviation from orthogonality.

## 5. Potential Spicity Functions Based on UNESCO EOS-80

This method is applied to find potential spicity function based on UNESCO EOS-80 equation of state (Unesco, 1981, 1983). In order to cover a wide range of salinity, the calculation is based on a tenth order polynomial. The Matlab program of the potential spicity function is in the form similar to the available Matlab code for calculating potential density, that is, it is in the form of  $sw\_pspi(s,t,p,pr)$ , where  $(s, t)$  is the in situ salinity (psu) and temperature ( $^{\circ}\text{C}$ ),  $p$  is the in situ pressure (db), and  $p_r$  is the reference pressure. These potential spicity functions are defined over the domain of  $\theta = [-2, 40]$  ( $^{\circ}\text{C}$ ) and  $S = [10, 40]$  (psu); the domain of definition is broad enough, so that these functions are applicable for oceanographic application in the open ocean, including the Arctic. For the convenience of application, we define potential spicity function at seven reference levels:  $p_r = 0, 500, 1,000, 2,000, 3,000, 4,000,$  and  $5,000$  (db), respectively.

In addition to the orthogonality constraint, the final definition of potential spicity function requires two additional constraints. First, we set the potential spicity to be zero at the mass center  $(\bar{S}, \bar{\theta})$  for each reference level, which is calculated from WOA09 data (Antonov et al., 2010), as listed in Table 1.

Second, the amplitude of the potential spicity satisfying the orthogonality is arbitrary; thus, we rescale the potential spicity function so that within the definition domain at each reference level, the averaged amplitude of the gradient ratio is  $\frac{|\nabla\pi|}{|\nabla\sigma|}^{core \ domain} = 1$ , where the core domain is defined as  $\theta = [0, 30]$  ( $^{\circ}\text{C}$ ) and  $S = [32.5, 37.5]$  (psu). With these two constraints, the potential spicity function is completely determined.



**Table 1**  
( $\bar{S}$ ,  $\bar{T}$ ) Based on WOA09 at Different Reference Pressure  $p_r$

$p_r$ (db)	0	500	1,000	2,000	3,000	4,000	5,000
$\bar{S}$ (psu)	34.5914	34.6567	34.5997	34.7311	34.7468	34.7336	34.7266
$\bar{T}$ (°C)	18.1534	7.3949	4.2768	2.3580	1.7434	1.4064	1.3184

Note. psu = practical salinity unit.

As the first example, the potential spicity function defined at sea surface pressure is shown in Figure 4a. It is readily seen that potential density and potential spicity contours are orthogonal. In particular, at low salinity and low temperature the thermal expansion coefficient is negative, thus the potential density contours are convex toward low salinity. As a result, the potential spicity contours in this vicinity are convex upward. Whether two families of contours are orthogonal or not may be hard to judge by naked eyes; thus, we calculate the angle deviation from the 90°, with results shown in Figure 4b. For this case the RMS of angle deviation from orthogonality is quite small at the value of 0.0009°. In fact, the largest errors appear along the edge and corners of the domain; however, within the interior of the domain, the angle deviation from orthogonality is on the order of 0.0001° only.

As discussed in Appendix A, such small deviation from orthogonality indicates that the errors in distance defined in terms of the  $\sigma - \pi$  coordinates are much smaller than the errors induced in the in situ salinity

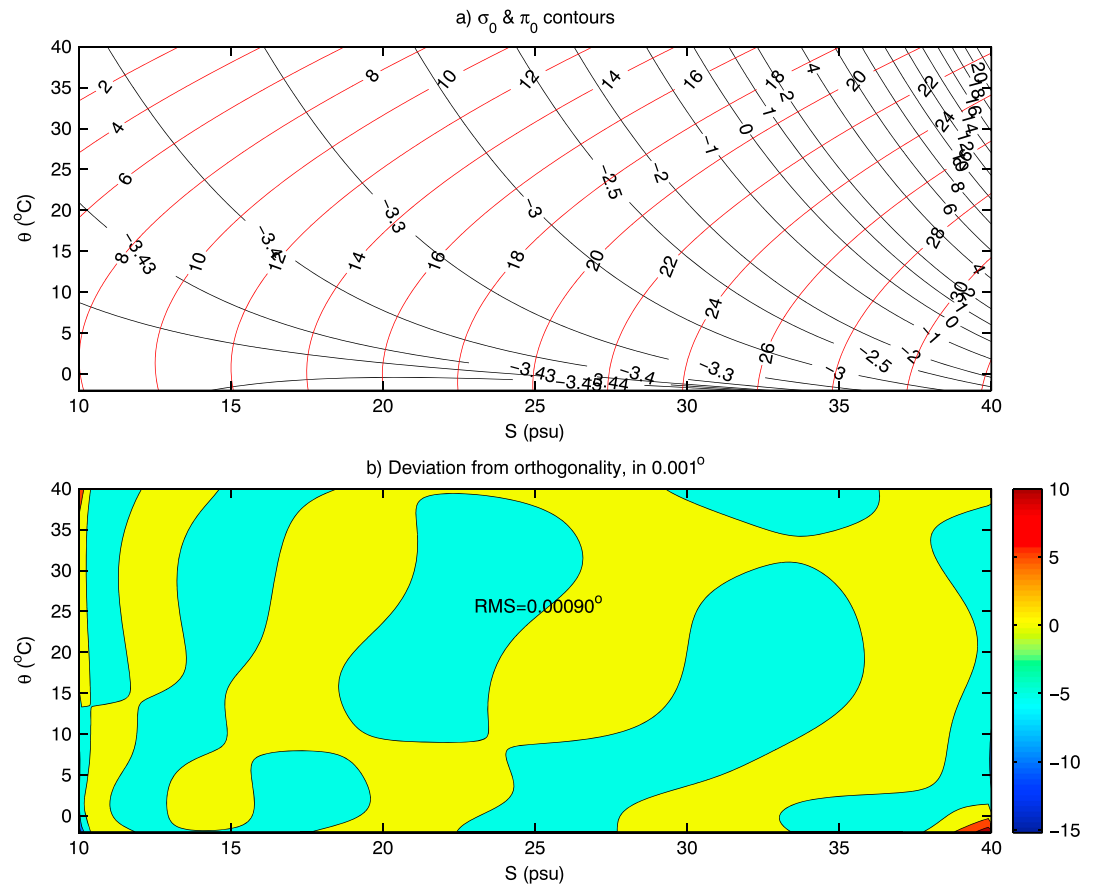


**Figure 4.** (a) Potential density ( $\sigma_0$ ) and potential spicity ( $\pi_0$ ) contours in the  $\theta - S$  plane over the definition domain of  $\theta = [-2, 40](^\circ\text{C})$ ;  $S = [10, 40](\text{psu})$ ; (b) angle deviation from orthogonality. RMS = root-mean-square; psu = practical salinity unit.

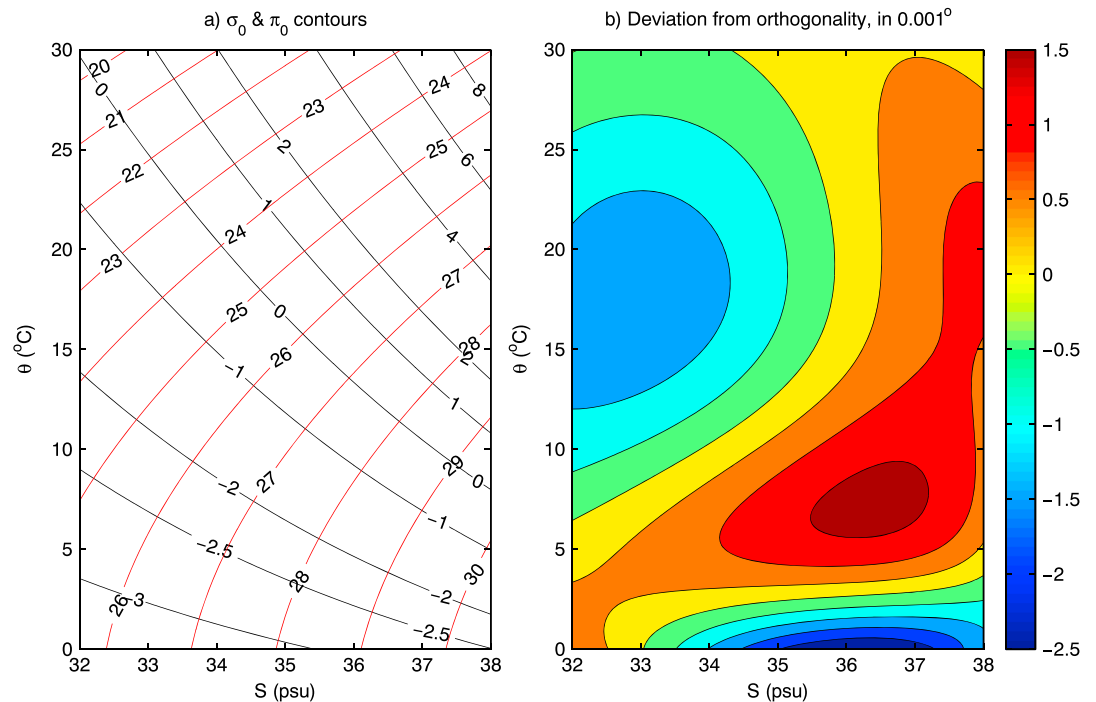


**Figure 5.** (a) Potential density ( $\sigma_0$ ) and potential spicity ( $\pi_0$ ) contours in the  $\theta - S$  plane over the domain of  $\theta = [0, 30](^{\circ}\text{C})$ ;  $S = [32, 38](\text{psu})$ ; (b) angle deviation from orthogonality. psu = practical salinity unit.

and temperature measurements; thus, the newly defined potential spicity function can be accepted as a nearly perfect orthogonal to the potential density.

The main domain of definition adapted in this study is  $\theta = [-2, 40](^{\circ}\text{C})$  and  $S = [10, 40](\text{psu})$ . However, away from the Arctic Ocean, most seawater is confined to a much smaller domain in the  $\theta - S$  space. Thus, a narrower domain  $\theta = [0, 30](^{\circ}\text{C})$ ;  $S = [32, 38](\text{psu})$  is defined, and this domain covers the most part of seawater in the open ocean application.

The basic feature of potential spicity within this domain is shown in Figure 5. As shown in Figure 5b, the largest error of angle deviation from the orthogonality is within  $0.0025^{\circ}$ . It is clearly indicated that potential spicity contours are orthogonal to the contours of potential density, with even small deviation from orthogonality. Such a potential spicity can be used to construct the orthogonal coordinates postulated above.

As the second example, the potential spicity function defined for the reference pressure of 2,000 db is shown in Figure 6. It is readily seen that potential density and potential spicity contours are orthogonal. At this case the RMS of angle deviation from orthogonality is quite small at the value of  $0.0001^{\circ}$ . As shown in Figure A1, the relative angle errors associated with distance defined in the  $\sigma - \pi$  coordinates are totally negligible.

## 6. Potential Spicity Functions Based on UNESCO TEOS\_10

The most updated equation of state is defined as UNESCO TEOS\_10 (McDougall & Barker, 2011). Accordingly, the suitable thermodynamic variables are the conservative temperature, denoted as  $\Theta$  ( $^{\circ}\text{C}$ ), and absolute salinity, denoted as  $S_A$  (g/kg). Similar to the case of UNESCO EOS-80, the definition of potential spicity function needs two additional constraints. First, we set the potential spicity to be zero at the mass center ( $\bar{\Theta}$ ,  $\bar{S}_A$ ) for each reference level, which is calculated from WOA09 data, as listed in Table 2.

In comparison with UNESCO EOS-80, potential spicity defined in UNESCO TEOS\_10 has angle deviation slightly larger, as shown in Figure A1. Nevertheless, these errors of angle deviation from the orthogonality

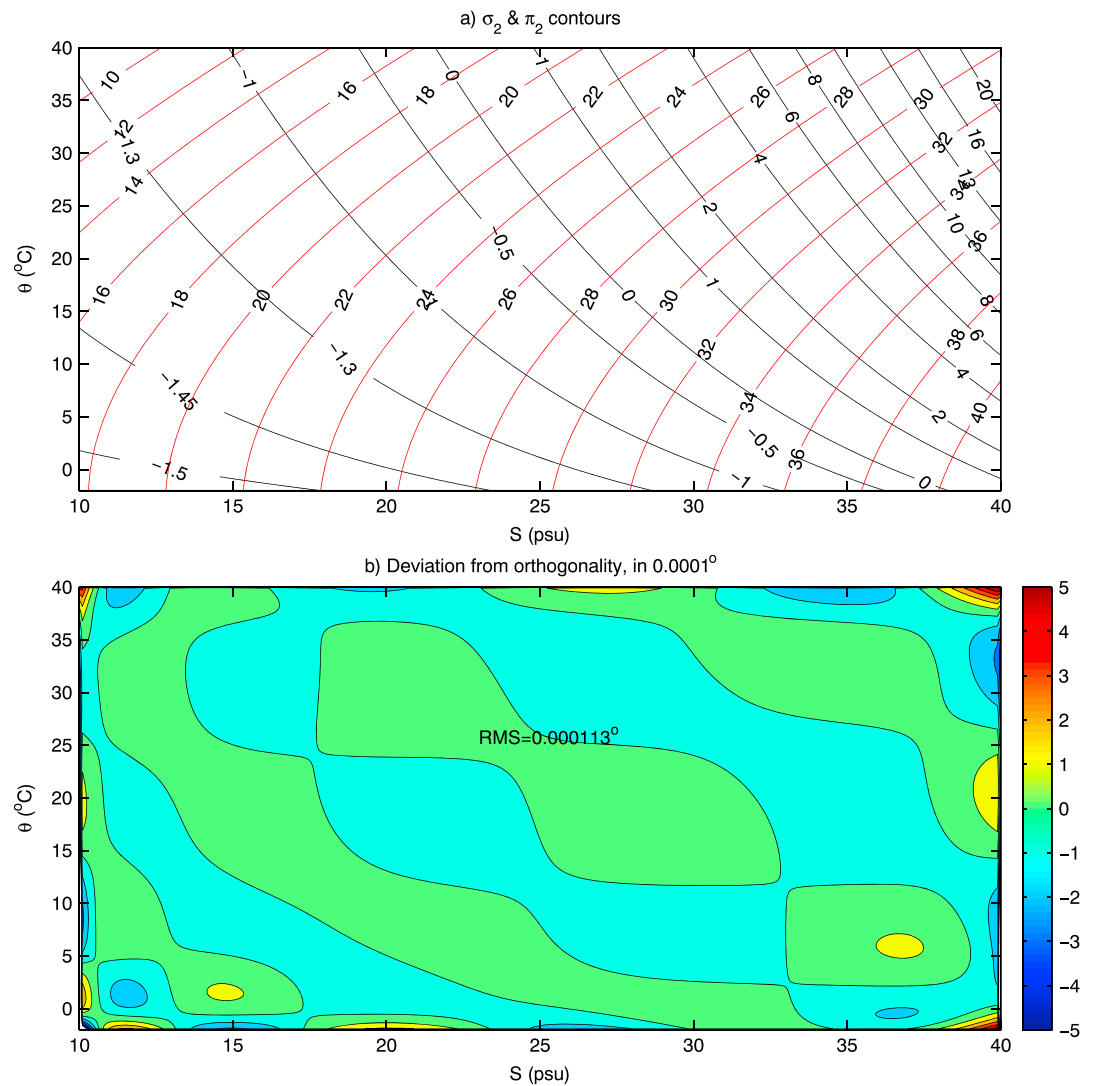


**Figure 6.** (a) Potential density ( $\sigma_2$ ) and potential spicity ( $\pi_2$ ) contours in the  $\theta - S$  plane over the definition domain of  $\theta = [-2, 40](^{\circ}\text{C})$ ;  $S = [10, 40](\text{psu})$ ; (b) angle deviation from orthogonality. RMS = root-mean-square; psu = practical salinity unit.

is quite small, and they are negligible compared to the relative errors associated those met in the in situ observations.

Following the currently used notation in the Matlab code based on TEOS\_10, the potential spicity function is defined in the form of  $\text{gsw\_pspi}(S_A, \Theta, p_r)$ , where  $(S_A, \Theta)$  is the absolute salinity (g/kg) and conservative temperature ( $^{\circ}\text{C}$ ) and  $p_r$  is the reference pressure (db). These potential spicity functions are defined over the domain of  $\Theta = [-2, 40](^{\circ}\text{C})$  and  $S_A = [10, 40](\text{g/kg})$ . For the convenience of application, we also define potential spicity at seven reference levels:  $p_r = 0, 500, 1,000, 2,000, 3,000, 4,000,$  and  $5,000$  (db), respectively.

**Table 2**  
( $\bar{S}_A, \bar{\Theta}$ ) Based on WOA09 at Different Reference Pressure  $p_r$

$p_r$ (db)	0	500	1,000	2,000	3,000	4,000	5,000
$\bar{S}_A$ (g/kg)	34.7552	34.8231	34.7693	34.9045	34.9219	34.9090	34.9031
$\bar{\Theta}$ ( $^{\circ}\text{C}$ )	18.1532	7.3420	4.1973	2.2145	1.5201	1.0894	0.8894

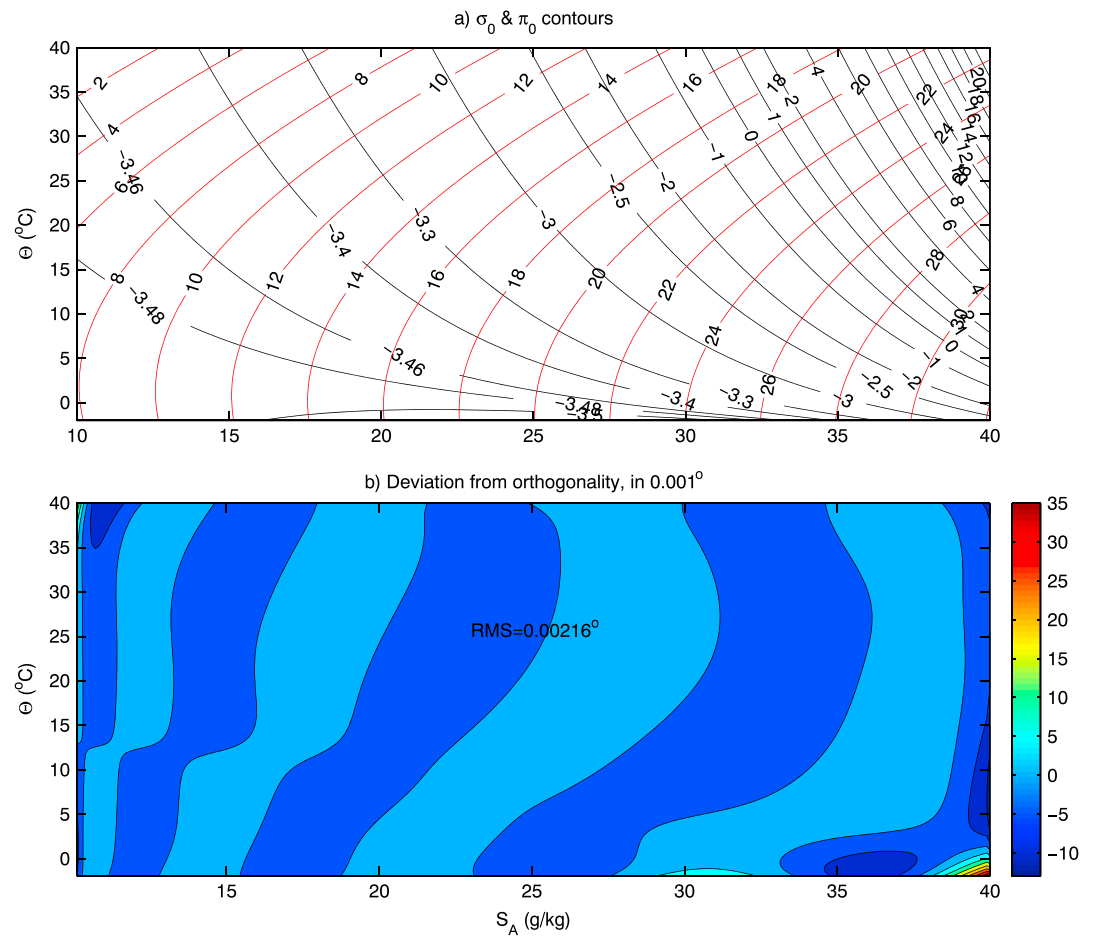


**Figure 7.** (a) Potential density ( $\sigma_0$ ) and potential spicity ( $\pi_0$ ) contours in the  $\Theta$ - $S_A$  plane over the definition domain of  $\theta = [-2, 40](^\circ\text{C})$ ;  $S_A = [10, 40](\text{psu})$ ; (b) angle deviation from orthogonality. RMS = root-mean-square.

As an example, we show the contours of  $\sigma_0$  and  $\pi_0$  defined at the surface pressure in Figure 7. It is readily seen that potential spicity contours are orthogonal to the potential density contours. The exact error of angle deviation from orthogonality is shown in Figure 7b. For this case the RMS error is about  $0.00216^\circ$ . Although this value is slightly larger than the corresponding value of  $0.0009^\circ$  defined in terms of UNESCO EOS-80, it is quite small and acceptable, as shown in Figure A1.

The basic feature of potential spicity within the narrower domain is shown in Figure 8. It is readily seen that potential spicity contours are orthogonal to the contours of potential density, with even smaller deviation from orthogonality.

## 7. Application of $\sigma - \pi$ Coordinates

With the introduction of potential spicity we now have a dual pair coordinate system, that is,  $\theta - S$  and  $\sigma - \pi$ . Thus, in addition to the traditional  $\theta - S$  diagram used in oceanography, one can also use the  $\sigma - \pi$  diagram for water mass analysis. An in-depth discussion of the meaning of potential spicity and the usage of the  $\sigma - \pi$  coordinates are beyond the scope of this paper, and will be presented in a separated publication.

As an example, we discuss the concept of radius of signal. In the traditional  $\theta - S$  plane, it is rather difficult to quantify how much the signal spreads because both axes are with different dimensions and the thermal expansion and haline contraction coefficients vary in the parameter space. With the introduction of this new (approximately) orthogonal curvilinear coordinates  $\sigma - \pi$ , the situation is quite different because now we can define the distance between two water parcels, with properties  $(\theta_1, S_1)(\theta_2, S_2)$ , or using the sea

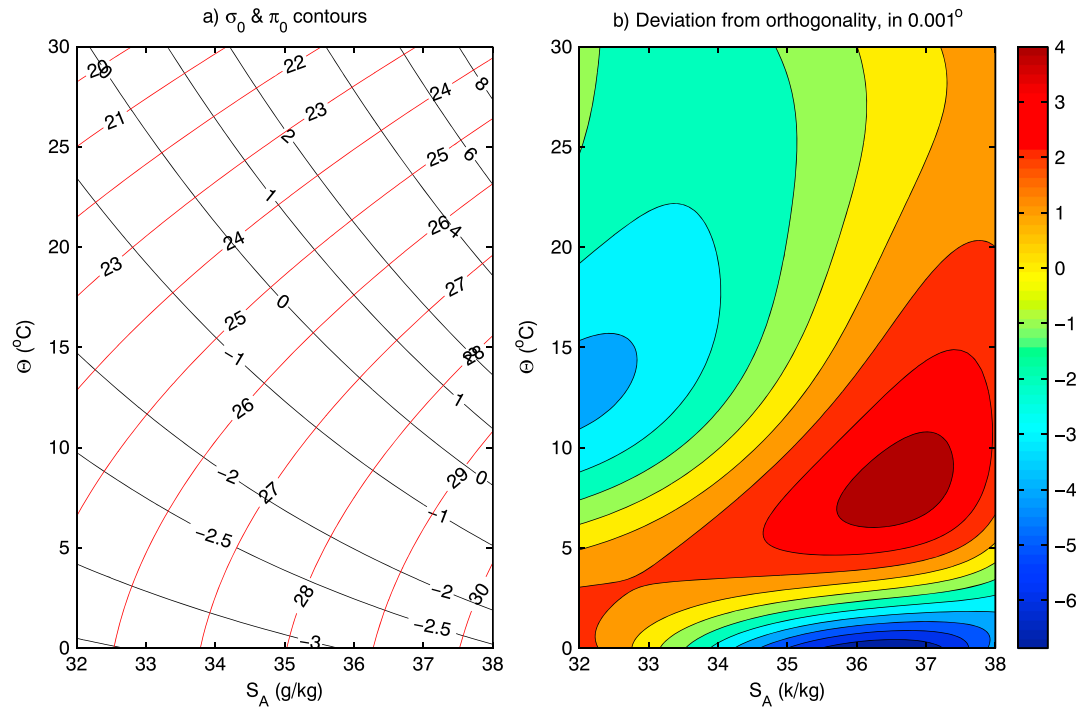


**Figure 8.** (a) Potential density ( $\sigma_0$ ) and potential spicity ( $\pi_0$ ) contours in the  $\theta$ - $S_A$  plane over the domain of  $\theta = [0, 30](^{\circ}\text{C})$ ;  $S_A = [32, 38](\text{g/kg})$ ; (b) angle deviation from orthogonality.

surface as the reference level equivalently we have  $(\sigma_{0,1}, \pi_{0,1})(\sigma_{0,2}, \pi_{0,2})$ . The corresponding distance between these two water parcels are

$$D_{1,2} = \sqrt{(\sigma_{0,1} - \sigma_{0,2})^2 + (\pi_{0,1} - \pi_{0,2})^2}. \quad (41)$$

A simple and vitally important application of the concept of distance is the radius of signal. First, from the original data point  $(\sigma_i, \pi_i)$  we calculate the mean potential density and potential spicity  $(\bar{\sigma}, \bar{\pi})$  corresponding to the mass center of signal. Then the radius of signal is defined in terms of contributions due to the root-mean square values of  $(\sigma_i - \bar{\sigma})$  and  $(\pi_i - \bar{\pi})$

$$R_s = \sqrt{[\text{rms}(\sigma_i - \bar{\sigma})]^2 + [\text{rms}(\pi_i - \bar{\pi})]^2}. \quad (42)$$

The radius of signal can be used to evaluate the data scattering.

Based on the monthly mean GODAS data (Behringer & Xue, 2004), provided by the NOAA-ESRL Physical Sciences Division, Boulder, Colorado, from their Web site at <https://www.esrl.noaa.gov/psd/>, we select two locations A ( $179.5^{\circ}\text{E}$ ) and B ( $100.5^{\circ}\text{W}$ ) along the equator ( $0.5^{\circ}\text{S}$ ). Both locations are at the depth of 145 m from 1980 to 2015. Since the location A is well above the equatorial main thermocline, its water mass properties (such as  $\theta$  and  $S$ ) carry strong variability related to ENSO events. As a result, the  $\theta$ - $S$  properties scatter greatly in the  $\theta$ - $S$  plane, as shown in Figure 9a. On the other hand, location B is near the eastern boundary and below the main thermocline at this location, the variability in water mass properties is much less affected by the ENSO processes; consequently, the water mass properties at location B vary much smaller amplitude than A, as shown in the upper panels of Figure 9. However, it is rather difficult to quantify the signal spreading in the traditional  $\theta - S$  diagram.

Using the  $\sigma - \pi$  coordinates, we can calculate the distance between two water masses and RMS distance from the center of mass. As shown in the lower panels of Figure 9, the radius of signal at location A is  $0.8665 (\text{kg/m}^3)$ , which is much larger than that at location B,  $0.2194 (\text{kg/m}^3)$ . This example demonstrates the usefulness of calculating the distance between water masses and the radius of signals.

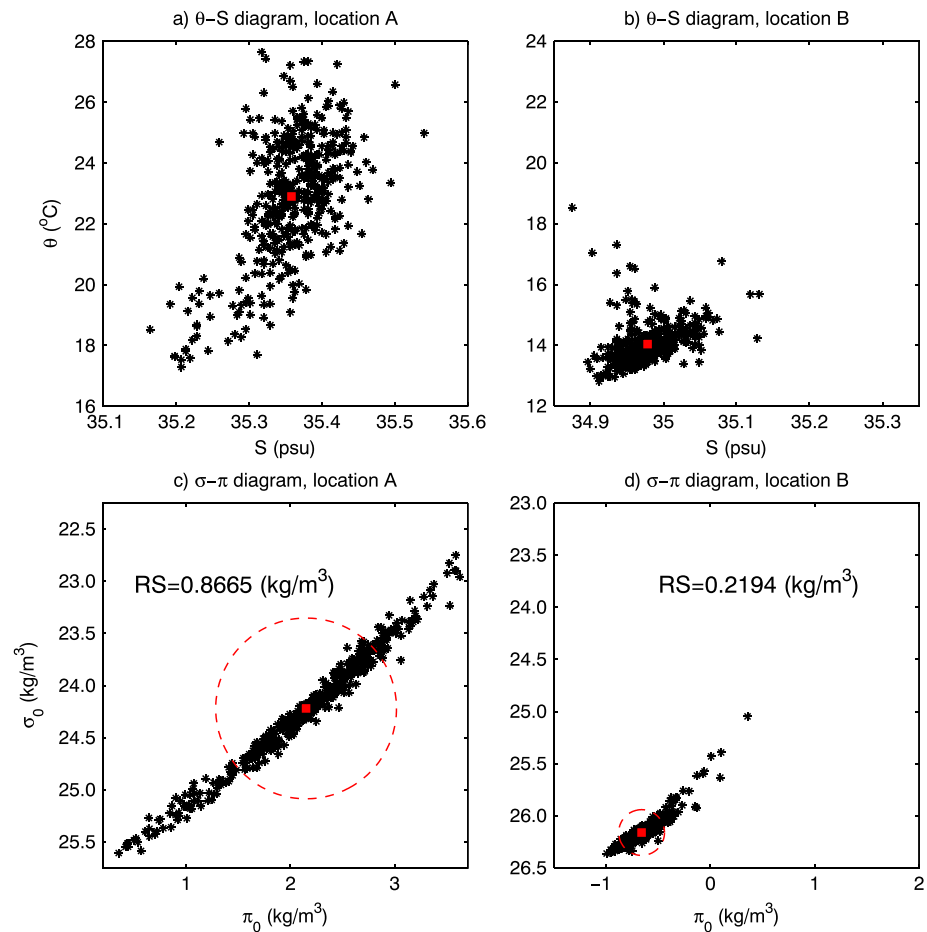


**Figure 9.**  $\theta - S$  (upper panels) and  $\sigma - \pi$  (lower panels) diagrams for two grid points taken at depth of 145 m along the equatorial ocean, with respective longitude of 179.5 (left panels) and 100.5°W (right panels), based on GODAS data. The red dots correspond to the mean values and the red circles refer to the radius of signal. psu = practical salinity unit.

## 8. Conclusion

It is possible to define a potential spicity function, whose contours are (in the least square sense) orthogonal to those of potential density. Introducing such functions opens up a new approach in oceanography. First of all, it can be combined with the potential density to form an orthogonal coordinate system. The  $\sigma - \pi$  diagram provides another diagnostic tool for water mass analysis in the world oceans; in particular, the orthogonality of the coordinate enables us to define the distance between water masses and thus the radius of signal and radius of the state. The physical meaning of such defined potential spicity and its application will be discussed in a separated paper. Due to the nonlinearity of the equation of state, if the local pressure is too far away from the reference pressure, potential density does not represent the stratification accurately, and the corresponding potential spicity may not be very accurate. Therefore, in application it is recommended that a reference pressure in the middle of the pressure range is chosen as the reference one.

## Appendix A: Errors in Distance Associated With Nonorthogonality

The errors in distance induced by nonorthogonality can be estimated as follows. In a nonorthogonal curvilinear coordinates  $(\chi, \eta)$ , the distance between two grid points is defined as

$$ds^2 = \Delta\chi^2 + \Delta\eta^2 - 2\Delta\chi\Delta\eta \cos\gamma, \quad (\text{A1})$$

where  $\Delta\chi$  and  $\Delta\eta$  are the infinitesimal arc length projected onto the coordinates axes and  $\gamma$  is angel between

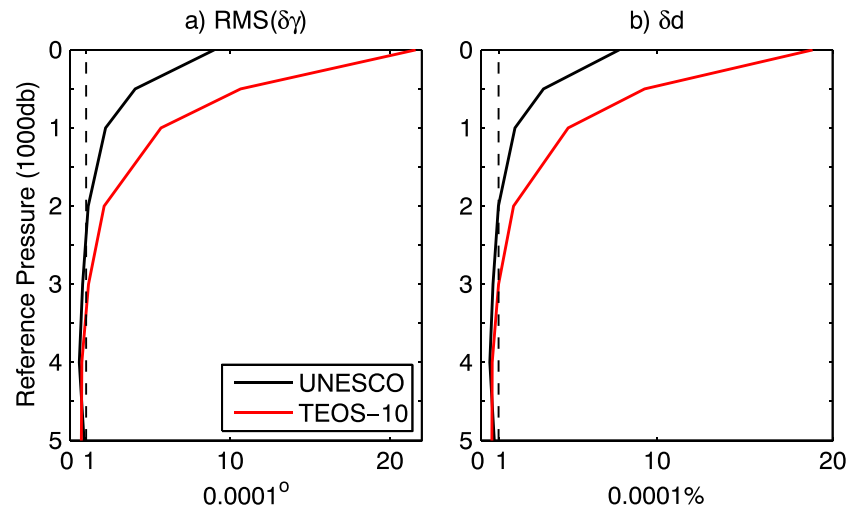


**Figure A1.** Errors estimates for potential spicity function defined in this study. (a) RMS of angle deviation from orthogonality; (b) relative error in distance. RMS = root-mean-square.

these two arc elements. Assume  $\Delta\chi = \Delta\eta = 1$  and denote angle deviation from orthogonality as  $\delta\gamma$ , then the distance is

$$ds = \sqrt{2(1 - \cos\gamma)} = \sqrt{2(1 - \sin\delta\gamma)}. \quad (\text{A2})$$

The second term is the off diagonal term in the matrix tensor. If we assume the coordinates are nearly orthogonal and thus omit this term, the nominal distance is  $ds_{nomi} = \sqrt{2}$ ; therefore, the relative error in distance is  $\delta r = \frac{ds_{nomi} - ds}{ds} \sim 0.5 \sin\delta\gamma \sim 0.5\delta\gamma$ . In terms of the commonly used unit of degree, the estimated relative error is approximately equal to  $\frac{\pi}{360}\delta\gamma \sim 0.00873\delta\gamma(^{\circ})$ .

Errors associated with field salinity and temperature observations are on the order of 0.001 (psu) and 0.001 °C. Assuming the normal range of salinity is 30–40 psu and the normal range of temperature is 0–40 °C; thus, the relative errors in potential density based on in situ salinity and temperature observation is on the order of 0.01%. Figure A1 shows clearly that error associated with the nonorthogonality induced by the definition of potential spicity is 10–100 times smaller than that induced in observation. Therefore, the error induced in the definition of potential spicity function is completely negligible.

#### Acknowledgments

We benefited from discussion with many of our colleagues, in particular Ray Schmitt. Yu and Zhou are supported by the National Natural Science Foundation of China (91752108 and 41476167), the National Natural Science Foundation of Guangdong Province, China (2016A030311042), and the Guangzhou Science and Technology Program key project (201804020056), and the Strategic Priority Research Program of the Chinese Academy of Sciences (XDA11030302). Our calculation is based on the commonly used Matlab UNESCO EOS-80 and TEOS\_10; in addition, both GODAS and WOA09 data were used in this study. The newly defined potential spicity functions in forms of standard Matlab codes are included in the supporting information.

#### References

- Antonov, J. I., Seidov, D., Boyer, T. P., Locarnini, R. A., Mishonov, A. V., Garcia, H. E., et al. (2010). World ocean atlas 2009. In S. Levitus (Ed.), *Salinity* (Vol. 2, p. 184). Washington, DC: NOAA Atlas NESDIS 69, U.S. Government Printing Office.
- Behringer, D. W., & Xue, Y. (2004). Evaluation of the global ocean data assimilation system at NCEP: The Pacific Ocean. *Eighth Symposium on Integrated Observing and Assimilation Systems for Atmosphere, Oceans, and Land Surface, AMS 84th Annual Meeting* (pp. 11–15). Seattle, Washington: Washington State Convention and Trade Center.
- Flament, P. (2002). A state variable for characterizing water masses and their diffusive stability: Spiciness. *Progress in Oceanography*, 54(1–4), 493–501. [https://doi.org/10.1016/S0079-6611\(02\)00065-4](https://doi.org/10.1016/S0079-6611(02)00065-4)
- Huang, R. X. (2011). Defining the potential spicity. *Journal of Marine Research*, 69(4), 545–559. <https://doi.org/10.1357/002224011799849390>
- Jackett, D. R., & McDougall, T. J. (1985). An oceanographic variable for the characterization of intrusions and water masses. *Deep Sea Research*, 32(10), 1195–1207. [https://doi.org/10.1016/0198-0149\(85\)90003-2](https://doi.org/10.1016/0198-0149(85)90003-2)
- Mamayev, O. I. (1975). *Temperature-salinity analysis of world ocean waters* (p. 384). Amsterdam-Oxford-New York: Elsevier Scientific Publishing Company.
- McDougall, T. J., & Barker, P. M. (2011). *Getting started with TEOS-10 and the Gibbs Seawater (GSW) oceanographic toolbox* (p. 28). SCOR/IAPSO WG127.
- McDougall, T. J., & Krzysik, O. A. (2015). Spiciness. *Journal of Marine Research*, 73(5), 141–152. <https://doi.org/10.1357/002224015816665589>
- Munk, W. (1981). Internal waves and small-scale processes. In *Evolution of physical oceanography* (pp. 264–291). Cambridge, MA: MIT Press.
- Stommel, H. (1962). On the cause of the temperature-salinity curve in the ocean. *National Academy of Science*, 48(5), 764–766. <https://doi.org/10.1073/pnas.48.5.764>
- Unesco (1981). The practical salinity scale 1978 and the international equation of state of seawater 1980. *UNESCO Technical Papers in Marine Science*, 36, 25.
- Unesco (1983). Algorithms for computation of fundamental properties of seawater. *UNESCO Technical Papers in Marine Science*, 44, 53.
- Veronis, G. (1972). On properties of seawater defined by temperature, salinity and pressure. *Journal of Marine Research*, 30, 227–255.